

18. Rozenberg G V *Usp. Fiz. Nauk* **69** (1) 57 (1959) [*Sov. Phys. Usp.* **2** 666 (1959)]
19. Rozenberg G V *Usp. Fiz. Nauk* **91** (4) 569 (1967) [*Sov. Phys. Usp.* **10** 188 (1967)]
20. Zege E P, Ivanov A P, Katsev O L *Perenos Izobrazheniya v Rasseyivayushchei Srede* (Image Transfer in a Scattering Medium) (Minsk: Nauka i Tekhnika, 1985) [Translated into English: *Image Transfer Through a Scattering Medium* (Berlin: Springer-Verlag, 1991)]
21. Ivanov A P *Optika Rasseyivayushchikh Sred* (Optics of Scattering Media) (Minsk: Nauka i Tekhnika, 1969)
22. Loiko V A, in *Rasseyaniye i Pogloshchenie Sveta v Prirodnykh i Iskusstvennykh Dispersnykh Sredakh* (Light Scattering and Absorption in Natural and Artificial Dispersed Media) (Ed. A P Ivanov) (Minsk: Inst. Fiziki im. B I Stepanova AN BSSR, 1991) p. 355
23. Evstrapov A A, Kurochkin V E *Opt. Zh.* **62** (2) 50 (1995)
24. Evstrapov A A, Kurochkin V E *Opt. Zh.* **62** (5) 40 (1995) [*J. Opt. Technol.* **62** 304 (1995)]
25. Kurochkin V E, Makarova E D *Analytical Commun.* **33** 115 (1996)
26. Burylov D A et al. *Zh. Analit. Khim.* **52** 551 (1997) [*J. Analytical Chem.* **52** 492 (1997)]
27. Bulyanitsa A L, Kurochkin V E *Avtomatika Telemekh.* (9) 187 (1999) [*Automat. Remote Control.* **60** 1368 (1999)]
28. Bulyanitsa A L, Kurochkin V E, Burylov D A *Radiotekh. Elektron.* **47** 343 (2002) [*J. Commun. Technol. Electron.* **47** 307 (2002)]
29. Bulyanitsa A L, Kurochkin V E *Nauchn. Priborostroenie* **12** (2) 30 (2002)
30. Tsypkin Ya Z, Polyak B T *Dinamika Sistem* (12) 22 (1977)
31. Bedel'baeva A A *Avtomatika Telemekh.* (1) 87 1978
32. Kurochkin V E, Evstrapov A A, Makarova E F "Opticheskoe ustroystvo dlya khimicheskogo analiza" ("Optical device for chemical analysis"), RF Patent 2157987, priority of 21.05.1996 (2000)
33. Fedorov A A et al. *Dokl. Ross. Akad. Nauk* **405** (1) 133 (2005) [*Dokl. Biochem. Biophys.* **405** 388 (2005)]

PACS numbers: 42.68.Wt, 95.55.Cs, 95.75.Qr

DOI: 10.1070/PU2006v049n09ABEH0006106

## Adaptive optical imaging in the atmosphere

V P Lukin

### 1. Introduction

As is well known, adaptive optics (AO) enjoys effective use in the formation of optical beams and images with the aim of concentrating laser beam energy, improving the sharpness of optical images, increasing the data transfer rate in optical communication lines, and solving other specific problems.

Investigations to develop methods and systems of adaptive optics are being pursued at the Laboratory of Coherent and Adaptive Optics of the Institute of Atmospheric Optics, Siberian Division of the Russian Academy of Sciences. This research is aimed at both elaborating the theory of adaptive systems and developing new elements, models of the systems, and their algorithms.

### 2. Problems in 'viewing' through the atmosphere

The bulk of information in astronomy is obtained by ground-based instruments. However, inhomogeneities of Earth's atmosphere (refraction, turbulence, radiation-absorbing gases, aerosols) seriously limit the capabilities of astronomical systems. In their papers in the late 1960s, Kolchinskii, Tatarski, and Frid formulated the atmosphere-imposed limitations on astronomical systems. Their results were obtained assuming the Kolmogorov–Obukhov model for

the fluctuation spectrum of the refractive index:

$$\Phi_n(\kappa, h) = 0.033 C_n^2(h) \kappa^{-11/3}, \quad \frac{1}{L_0} \ll \kappa \ll \frac{1}{l_0}.$$

Here,  $C_n^2(h)$  is the structure parameter of the atmospheric refractive index,  $h$  is the current height above the underlying surface in the atmosphere,  $\kappa$  is the wavenumber for turbulent inhomogeneities, and  $L_0$  and  $l_0$  are the inner and outer turbulence scales.

Solving the problem of the optical wave propagation through randomly inhomogeneous media has shown that the phase structure function at a distance  $\rho$  obeys the five-thirds power law:

$$D_S(\rho) = 2.91 k^2 \int_0^\infty dh C_n^2(h) \rho^{5/3},$$

where  $k = 2\pi/\lambda$  and  $\lambda$  is the radiation wavelength. Proceeding from the last expression, the so-called atmosphere coherence radius  $r_0$  was introduced:

$$D_S(\rho) = 2.91 k^2 \int_0^\infty dh C_n^2(h) \rho^{5/3} = 6.88 \left( \frac{\rho}{r_0} \right)^{5/3},$$

which determines the limiting angular resolution  $\gamma_0 = \lambda/r_0$  of an optical system in the turbulent atmosphere, the Strehl parameter  $St = \exp(-\sigma^2)$  of the astronomical system atmosphere–telescope (where  $\sigma^2$  is the variance of phase distortions), the optical transfer function, the point spread function, and other parameters of the astronomical instrument.

Research carried out in the 1960s showed that these theoretical results agree nicely with experimental data obtained for optical apertures of the order of 2–4 m. However, the effective apertures of ground-based astronomical telescopes began to increase swiftly: the 6 m BTA telescope (the Large Azimuth Telescope), the Multiple Mirror Telescope (MMT) with a matrix of six 8 m apertures, the 3.6 m New Technology Telescope (NTT), the 10 m Keck telescope, the 8.2 m Very Large Telescope Interferometer (VLT), and the 8 m Subaru telescope made their appearance. In this connection, interest was aroused in the study of the phase fluctuations of optical waves in wide-aperture reception.

### 2.1 Phase fluctuations of optical waves in a turbulent atmosphere

The 1970s saw the development [1, 2] of interference wave phase meters in the optical range for the investigation of turbulent phase fluctuations of the optical wave for long spatial and temporal delays. The phase structure function was found to be sensitive both to the turbulence intensity and to the outer turbulence scale. This compelled reconsidering Tatarski's and Frid's results. In the early 1970s, measurements were made of optical wave phase fluctuations in the USSR (V Pokasov, V Lukin), Italy (L Ronchi, A Consortini), and the USA (G Ochs, S Clifford), with the result that the effect of 'phase structure function saturation' was discovered almost simultaneously [1, 2]. In Refs [1, 3, 4], this effect was interpreted and invoked to describe the spectrum of turbulence with a finite outer scale. We recall that the outer turbulence scale in the Kolmogorov–Obukhov model is assumed to be infinite.

In the 1970s and the 1980s, a consistent theory [1, 2] of phase fluctuations for optical waves propagating through a

turbulent atmosphere was elaborated with the use of turbulence spectra with a finite outer scale:

$$\Phi_n(\kappa, h) = 0.033 C_n^2(h) (\kappa^2 + \kappa_0^2)^{-11/6}, \quad \kappa_0 = \frac{2\pi}{L_0},$$

$$\Phi_n(\kappa, h) = 0.033 C_n^2(h) \kappa^{-11/3} \left[ 1 - \exp\left(-\frac{\kappa^2}{\kappa_0^2}\right) \right].$$

Calculations were made of the statistical characteristics of phase fluctuations (variance, correlation functions, spectra, structural function) as the principal distorting factor for imaging systems. It turned out that the variance of image tremor is described [2] by the formula

$$\sigma^2 \approx \int_0^\infty dh C_n^2(h) \left[ (2R)^{-1/3} - \left( \frac{1}{4R^2} + \kappa_0^2 \right)^{1/6} \right],$$

where  $2R$  is the telescope aperture, whence it is clear that the outer scale begins to exert an effect on the image tremor even when the telescope aperture does not exceed 0.01 of the value of the outer turbulence scale.

As a result, the integral characteristics of astronomical instruments were shown to greatly depend on the astroclimatic characteristics of the atmosphere, among which is the outer turbulence scale. More recently, by using the measurement data of optical wave fluctuations for atmospheric propagation paths, it has been possible to reconstruct the outer turbulence scale and relate its magnitude to the level of thermodynamic atmospheric stability [2].

## 2.2 Astroclimatic measurements

Our calculations and our theory enabled developing new atmospheric turbulence meters. Several phase fluctuation meters were made for the optical region, in particular, IFAS (analog tracking phase meter), which was tested in 1970–1976, IFUP (angle-of-arrival fluctuations meter), which passed tests on the BTA [2, 3] in 1979–1983, and DIT (differential turbulence meter), which passed tests on the Big

Solar Vacuum Telescope (BSVT) in 1996–1999. These systems operated with both laser radiation and the emission of bright (+4) stars (Fig. 1).

The experimental data obtainable with the aid of these devices enable estimating both the atmospheric coherence radius  $r_0$  and the outer turbulence scale  $L_0$ . This permitted more accurately determining the atmospheric astroclimate parameters in several regions of Russia: in the Northern Caucasus (Special Astrophysical Observatory), near Lake Baikal (Baikal Astrophysical Observatory), and in the south of the Irkutsk District (Mondy Observatory).

## 2.3 Effective external scale

In 1997, based on the analysis of astroclimatic measurement data, we introduced the notion of the ‘effective outer turbulence scale’ [4] for the atmosphere as a whole. The effective outer turbulence scale is introduced as an approximation of the value of the phase structure function  $D_S(\rho, C_n^2(h), L_0(h))$ , which is calculated using models or the data of direct measurements of the vertical evolution of the turbulence level  $C_n^2(h)$  and the outer scale  $L_0(h)$ . The approximation amounts to setting

$$D_S(\rho, C_n^2(h), L_0(h)) = D_S(\rho, C_n^2(h), L_0^{\text{eff}}),$$

i.e., to a different calculation of the structure function: the profile  $C_n^2(h)$  is specified according to the model of vertical evolution and the outer scale is assumed to be constant,  $L_0(h) = L_0^{\text{eff}}$ . This permitted zoning all observatories in the world by the magnitude of the parameter  $L_0^{\text{eff}}$ . Part of the data are collected in Table 1. At present, this atmospheric parameter, which is a real characteristic of the site of an astronomical instrument, is commonly used. For the world’s best observatories,  $L_0^{\text{eff}}$  ranges between 10 and 30 m [4].

## 2.4 Development of the theory of anisotropic turbulence

The characteristics of atmospheric turbulence in a surface layer with a plane underlying the surface is adequately

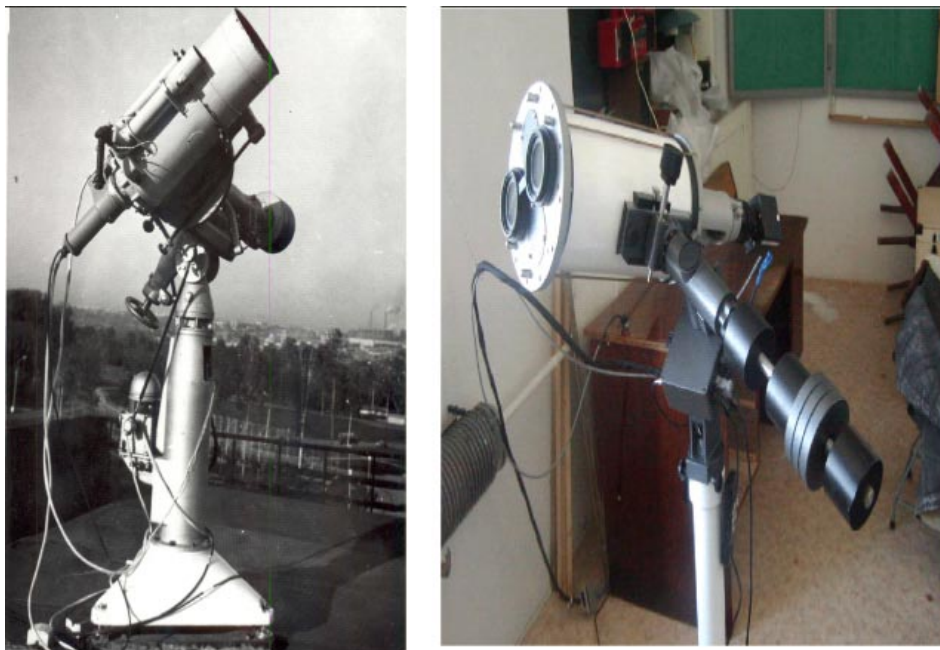


**Figure 1.** Photometric image tremor measuring instruments for astronomical phenomena: IFUP (a) and DIT (b).

**Table 1.** Comparison of the measurement data for the external turbulence scale.

Year	Author	External scale, m	Measuring instrument	Measurement site
1983	V P Lukin et al.	8–15	Telescope with a 60 cm aperture	Special Astrophysical Observatory (SAO), Russia
1984	Marriotti et al.	8	I2T interferometer	Geodynamical and Astronomical Research Center (CERGA), France
1987	Colavita et al.	> 200	'Mark III' stellar interferometer	Mount Wilson Observatory, USA
1989	Tallon	5–8	Hartmann–Shack wavefront monitor	Mauna Kea Observatory, USA
1991	Rigaut et al.	50	'Come-on' adaptive system	La Silla Observatory, Chile
1991	Nightingale	2	Differential image tremor monitor DIMM	La Palma Observatory, Spain
1993	Ziad et al.	5–100	Hartmann–Shack wavefront monitor	Haut-Provence Observatory, France
1994	Agabi et al.	50–300	GSM1 image tremor meter	Cote d'Azur Observatory, France
1995	Busher et al.	10–100	'Mark III' stellar interferometer	Mount Wilson Observatory, USA
1995	Fuchs	1.5–2.4	Pilot-balloon-assisted measurements	European Southern Observatory, Cerro Paranal, Chile

described by the Monin–Obukhov similarity theory. In such an isotropic layer, the Monin–Obukhov scale is constant for the whole territory. But above a mountainous relief, stable vortices emerge, and the Monin–Obukhov scale cannot be assumed to be constant in this case. In atmospheric optical research, especially in research into the effect of turbulence on the quality of optical images, we quite often have to deal with an anisotropic boundary layer in the mountains. Therefore, the development of a turbulence theory applicable directly to mountainous conditions has been of interest.

By invoking semiempirical hypotheses of the turbulence theory, we established [5] theoretically and experimentally that the Monin–Obukhov similarity theory in an arbitrary anisotropic layer is fulfilled locally, in the neighborhood of each point in the layer. Consequently, an arbitrary anisotropic layer is locally weakly anisotropic. The main parameter of turbulence in such a layer is the variable Monin–Obukhov number.

The theoretical and experimental data for the Tatarski outer scale  $L_0^T$  in the mountainous boundary layer in the Lake Baikal region are compared in Fig. 2. A comparison of the  $L_0^T$  scales measured in three different ways (by Tatarskii's definition, from saturation using spectra, and from the 5/3 dependence using spectra) shows that the results of experiments and the semiempirical theory for an anisotropic boundary layer are in satisfactory agreement [5, 6].

### 3. Development of the theory and practice of atmospheric adaptive systems

In 1977, we began investigating the feasibility of applying phase correction to reduce the atmospheric effect on the parameters of optical systems. The elaboration of the theory of atmospheric adaptive optical systems [2, 6] was substantially completed during the 1984–1986 period. The main results were published in the monograph Ref. [2] (1986), which was translated into English and published in the USA in 1996. We emphasize the most significant results.

Reference [6] (1979) for the first time described two-color adaptive systems for which the wavelengths of the main and reference radiation do not coincide.

Using the optical signal scattered from atmospheric irregularities for producing the reference signal was first proposed in Refs [7, 8]. In our first publication devoted to this question, which dates back to 1979, calculations were made of the cross-correlation function for the phase fluctuations of a Gaussian beam and the plane reference wave. Lukin and Emaleev [7] came up with the idea of employing the signal of backscattering from atmospheric irregularities for image correction. Lukin and Matyukhin [8] calculated the max-

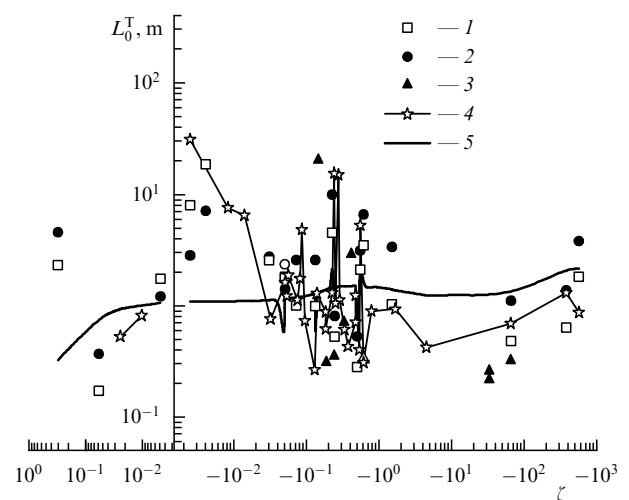


**Figure 2.** Comparison of experimental and theoretical data for the outer turbulence scale  $L_0^T$  in a mountainous anisotropic boundary layer;  $\zeta$  are the dimensionless Monin–Obukhov numbers calculated from the data of weather stations. The experimental data were obtained from the 5/3 power-law dependence using spectra (1), from saturation using spectra (2), and from Tatarskii's definition (3). Curve 4 corresponds to the semiempirical theory for an anisotropic layer and curve 5 to the semiempirical theory for an isotropic layer.

imum image correction attainable in a telescope with the use of a reference source formed at a fixed distance in the atmosphere.

Today, this research has received wide acceptance, and a new scientific area has emerged: the production and application of laser reference stars.

Using statistical fluctuation prediction was first proposed for the study of the dynamic properties of adaptive systems. Zuev and Lukin [9] analyzed the adaptive systems as dynamic systems. Apart from conventional permanent-lag adaptive systems, the capabilities of ‘fast’ systems as well as of ‘predictive’ adaptive systems were considered. The longest permissible time delays that ensure the requisite correction level for adaptive systems were determined. It was found that they are defined by the effective wind speed, the atmospheric coherence radius, and the parameters of the optical system.

During the same period, principles were elaborated and prototypes were made [8, 10–14] of the individual components of an adaptive optical system: compound multicomponent mirrors, mirrors for the fast control of the wavefront tilt, flexible bimorph optical elements, dissector and coordinate-sensitive photodetector tracking systems. Using the prototypes of the individual components of adaptive systems, experiments were carried out [7] in the phase correction of turbulent and refractive distortions in optical imaging and the formation of laser beams in the atmosphere in 1981.

#### 4. Adaptive optical system for telescopes

In 1993–1994, under the task of the Ministry of Science of the Russian Federation, an adaptive optical system was developed for the AST-10 telescope (Russian project of an adaptive compound 10-meter telescope). The telescope itself, which has a compound 91-element mirror, turned out to be too slow for real-time compensation of turbulent distortions. That is why, proceeding from an analysis of world experience in the

development of suchlike systems, a correction concept was proposed, which employed an adaptive secondary mirror. The entire optical system of the telescope was modeled, beginning with errors in the alignment of its primary mirror [15–18]. A telescope scheme proposed during the execution of the project comprised an adaptive secondary mirror and a mirror controllable in two angles to stabilize the image as a whole.

Also investigated were the feasibility of partial phase correction of the image with the aid of an adaptive secondary mirror, different turbulence levels on the basis of atmospheric models, different types of active mirrors (compound, flexible, and mode mirrors), and different wavefront measuring instruments [15–19]. We studied the effect of misphasing the AST-10 primary mirror by the magnitude of the Strehl parameter.

The telescope’s point spread function was calculated for a partial correction of turbulent distortions. Both compound and flexible mirrors with a different number of constituent elements were considered. Also investigated was the effect of the fluctuation of the number of photons in the incoming light flux during adaptive system operation with the radiation of faint stars. The operational capabilities of the telescope were calculated in the case where a laser reference star is used [18–20].

A study was made of the effect of a turbulent atmosphere on the signal in long-base interferometers, including stellar interferometers. The phase difference spectra were calculated analytically and numerically for the signals in stellar interferometers with different bases for different orientations of the wind velocity vector and the interferometer base, different turbulence spectra and wind speed models being used in this case [18]. Figure 3 shows the spectra of the phase difference in stellar interferometers with different bases: 3, 12, 38, and 85 m. The solid and dashed curves correspond to the longitudinal and perpendicular mutual orientations of the interferometer base and the wind velocity. Therefore, choosing the adequate

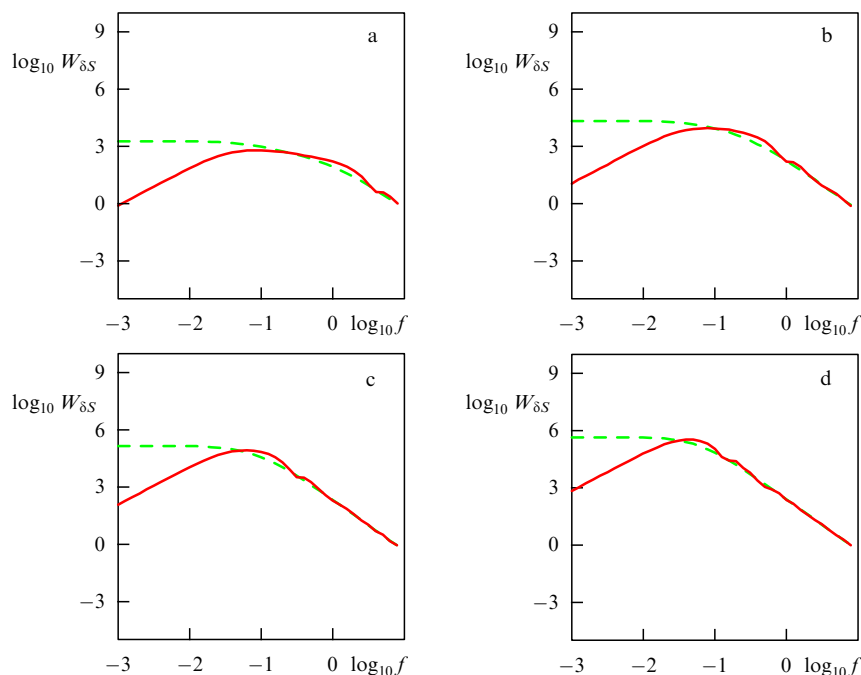


**Figure 3.** Frequency spectra  $W_{\delta S}(f)$  of phase difference fluctuations  $\delta S$  for interferometers with different bases: (a) 3 m, (b) 12 m, (c) 38 m, (d) 85 m;  $\delta S$  is a dimensionless quantity, the frequency  $f$  is measured in Hertz.

model for the altitude curve of the outer turbulence scale has been shown to be of paramount importance.

## 5. Adaptive solar telescope

We made an attempt to apply an AO system to the BSVT of the Institute of Solar–Terrestrial Physics, Siberian Division of the Russian Academy of Sciences. The first season was devoted to the collection of data on the daytime astroclimate of the Lake Baikal region. The DIT (differential image tremor) monitor of our design was used (see Fig. 1). The behavior of solar image distortions arising from the characteristic properties of this region was investigated. On this basis, the first-version AO system for the BSVT was developed [20]. Its task is to afford the operation of the system when a contrast ‘spot’ or a ‘pore’ is within the field of view of the wavefront monitor (Fig. 4a).

The prototype of the AO system, which comprised a device for measuring the displacement of the image center-of-gravity, stabilized a fragment of the solar image. A spot (a pore) on the solar surface was selected as the element for tracking. The image quality was improved by a factor of 4–16. Use was made of a two-coordinate-controllable mirror (Fig. 4b) with a piezoceramic drive (two such mirrors were delivered to the Nanjing Astronomical Instruments Research Center in China).

The adaptive system test data showed that the system was highly efficient during operation with a contrasting subject. Further progress in this direction involves the development of the prototype of an image displacement monitor with a capacity for work in conditions of small intensity variations. During the test operation of the adaptive optical system at the BSVT in 2004 and 2005, the contrast of the granulation pattern in different regions of the solar disk ranged between 1% and 4% on average (Fig. 5). In operations with a low-contrast image, a correlation algorithm for measuring image fragment displacements was used. The latest version of our adaptive system is employed to measure the image displacement of the solar granulation pattern on the basis of a modified correlation tracking algorithm [22]. Figure 6 displays persistent stabilization of a surface fragment of the solar surface. The image contrast for a ‘long’ (2 s) exposure in the tracking mode remains almost the same as for a ‘short’ (2 ms) exposure.

As a development of the above activities, we proposed the ‘Angara’ adaptive correction system for the correction of higher-order wavefront aberrations, which comprises a flexible multielement mirror and a wavefront monitor.

## 6. Laser guide stars

Laser guide stars (LGSs) are used in astronomy because the energy of radiation of weak stars is too low to furnish simultaneous operation of adaptive systems and the telescope itself. In work dating back to 1979–1980 [2, 8], it was shown for the first time that the backscattering signal from atmospheric irregularities can be used as a reference beacon. Several scientific experiments were carried out in the Astrofizika Research and Production Association and in our laboratory. Their results were published in the open press in the USSR and abroad. Meanwhile, a start on similar research in the USA was made in approximately 1982, and this research was classified until 1993.

Despite the attractiveness of the LGS technique, it suffers from one major disadvantage: there is practically no way of correcting the general slope of the wavefront. This problem



**Figure 4.** (a) Detail of a solar surface image in the BSVT. (b) Correcting mirror.

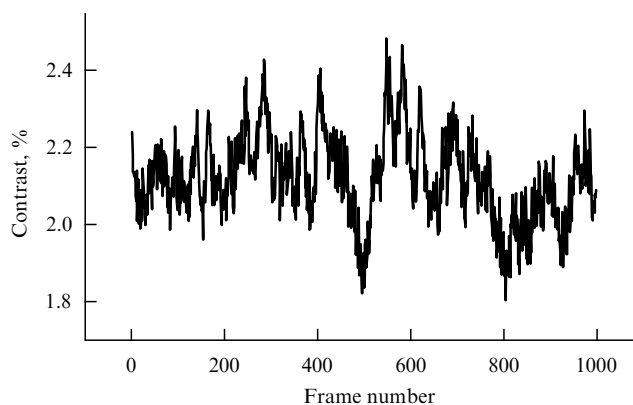


**Figure 5.** Contrast of a solar granulation image near a spot measured at the primary focus of the telescope. The detector field of view measures  $29 \times 29$  arc seconds.

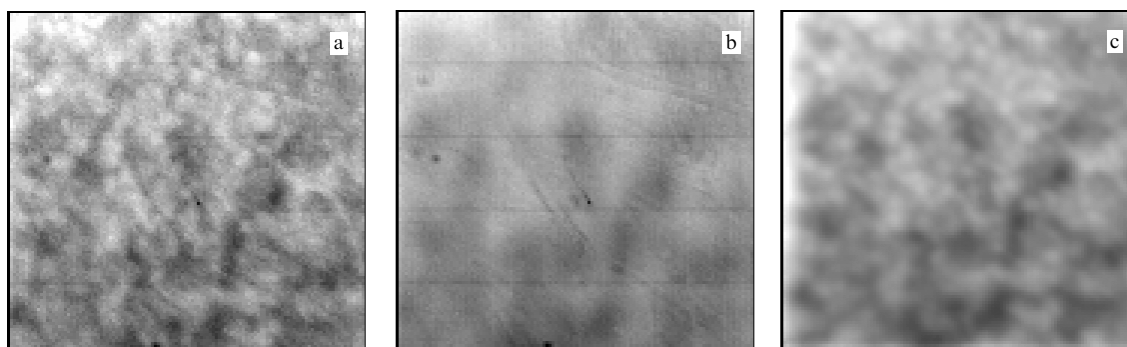


**Figure 6.** Photographs of the granulation image obtained (a) in the mode of short exposure (2 ms), (b) in the ‘long exposure’ mode (2 s) without control, and (c) in the ‘long exposure’ mode (2 s) with a modified correlation monitor.



has been stated in several papers, including our 1996 papers [17–19]. One possible way to solve this problem [17, 18, 21–23] involves using the optimal correction algorithm, which minimizes the residual distortions of the wavefront tilt arising from fluctuations. The gist of this algorithm consists in scaling the measurement data for the location of an LGS image with the aid of a weighting coefficient obtained either by calculations or by direct measurements.

We have proposed a hybrid scheme, which is free of several drawbacks of the previous analogs, and a new approach to the dynamic formation of LGSs. We have shown that using an LGS in the form of a reference cross produced by scanning two narrow laser beams affords efficient correction of wavefront tilts even for wide-aperture telescopes [21, 22].

## 7. Phasing of compound mirrors

The use of a large compound primary mirror in a telescope brings the additional problem of phasing the multielement compound mirror with an optical accuracy. We considered the distortions in a ground-based telescope caused by misphasing of the segments of the primary mirror [22–24]. The corresponding decrease in the Strehl parameter may be judged by Fig. 7, which allows comparing the data of a numerical experiment with the results of theoretical investigations. One can see that random displacements and tilts of mirror segments result in significant image distortions. In particular, under displacements with a variance of the order of one wavelength, the Strehl parameter decreases by a factor of five or more in comparison with the diffraction-limited value. The correction of random segment shifts with an amplitude of several hundred wavelengths is normally effected with the aid of capacitive or inductive surface sensors. At the same time, it is possible to compensate for displacements on the basis of purely optical techniques. An interference criterion based on a reference interference pattern was used as the goal control function. In the initial stage of investigations, the following optical arrangement was

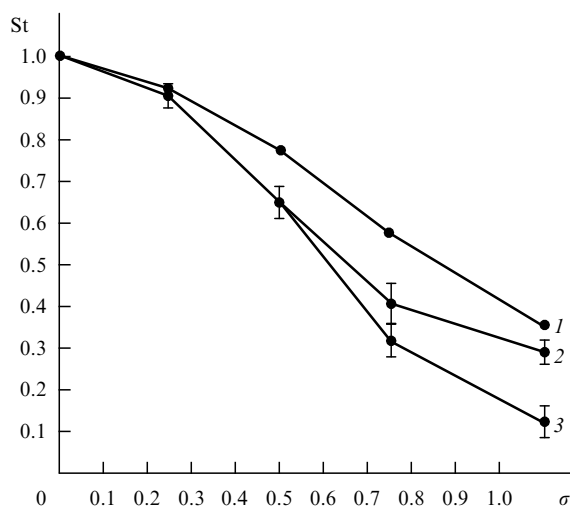


**Figure 7.** The strehl parameter as a function of the random-shift variance normalized by the radiation wavelength: theoretical results (curve 1) and data derived from a numerical experiment for a mirror with the number of segments  $32 \times 32$  (curve 2) and a mirror with the number of segments  $8 \times 8$  (curve 3).

used for this purpose. Special reflective plates were affixed at the interfaces between the segments. The center-of-gravity positions of the beams reflected from each of the plates were recorded in the plane of observation. Their displacements were determined to permit evaluation of random shifts of the segments. The determination of the shifts was followed by their compensation, which was either automatic, for instance with the use of the aperture probing algorithm, or by manual alignment.

Simple estimates show that a relative segment shift of  $10 \mu\text{m}$  results in a centroid displacement by the distance  $\Delta z$  about  $0.1 \text{ mm}$  in the plane located at the distance  $1 \text{ m}$  from the segmented mirror surface. In the calculations, the longitudinal dimension of the plates was assumed to be about  $1 \text{ cm}$ . The above displacement can be reliably recorded by modern digital video cameras. It may therefore be concluded that the proposed algorithm enables phasing the compound mirror surface with an accuracy of  $1\text{--}2$  wavelengths even when the initial relative shift is far greater than the wavelength.

We proposed a phasing algorithm allowing us to decrease the residual shifts of mirror segments to values far less than the optical radiation wavelength. Coherent beams produced by a laser source were reflected from two neighboring elements and directed to a common spot by beam-deflecting mirrors. Recorded in the plane of observation was an interference pattern, in which the fringe positions were determined by the relative phase shift of the beams. To bring the elements into phase, the aperture probing algorithm was used with the beams controlled only in one coordinate.

In this case, the interference criterion constructed with the use of the reference interference pattern was chosen as the goal function. Early in the investigation, the segments were brought into phase at the wavelength  $\lambda = 0.8 \mu\text{m}$ . Numerical experiments showed that the algorithm under consideration enabled compensating for the segment misphasing when the initial shifts were smaller than the wavelength,  $\Delta z = 0.367 \mu\text{m}$ . When the shift exceeds half the wavelength, the algorithm diverges, which results in an increase in segment shifts. The admissible range in initial shifts can be broadened by introducing an additional wavelength into the control algorithm. In particular, the values of the criterion calculated for different relative segment shifts for the wavelengths  $\lambda = 0.6$  and  $\lambda = 0.8 \mu\text{m}$  are given in Fig. 8. It can be seen from Fig. 8 that physical segment shifts of the same length give different phase shifts for different wavelengths. The peaks of the criteria coincide only for the shifts  $\Delta z = 0$  and  $\Delta z = 2.4$  ( $-2.4$ )  $\mu\text{m}$ . The range of shifts that can be compensated is additionally broadened by selecting the

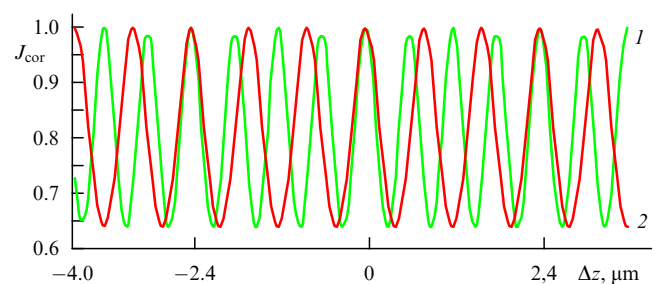


**Figure 8.** Correlation criterion  $J_{\text{cor}}$  versus relative shift  $\Delta z$  of mirror segments. Curve 1 corresponds to a wavelength  $\lambda_1 = 0.6 \mu\text{m}$  and curve 2 to a wavelength  $\lambda_2 = 0.8 \mu\text{m}$ .

**Table 2.** Maximum permissible shift  $\Delta z$  whereby the mirror surface can be phased in.  $\lambda_i$  are the wavelengths at which the control is effected.

$\lambda_1, \mu\text{m}$	$\lambda_2, \mu\text{m}$	$\lambda_3, \mu\text{m}$	$\Delta z, \mu\text{m}$
0.8	—	—	0.36
0.6	—	—	0.26
0.6	0.8	—	2.34
0.7	0.8	—	5.55
0.6	0.7	0.8	33.4

wavelengths of the interfering beams. Finally, the range may be radically broadened by introducing the third wavelength. Numerical experiments showed that the phasing for  $\lambda_1 = 0.6$ ,  $\lambda_2 = 0.7$ , and  $\lambda_3 = 0.8 \mu\text{m}$  is effected for the initial shift  $\Delta z = 2.34 \mu\text{m}$ . The data characterizing the admissible range of the shifts are collected in Table 2.

In conclusion, we summarize the work of the Institute of Atmospheric Optics, Siberian Division of the Russian Academy of Sciences, on the problem of the application of atmospheric optics for the improvement of viewing through the atmosphere as a randomly inhomogeneous medium. The proposed techniques and the prototypes of the corresponding systems have successfully passed laboratory and full-scale tests to demonstrate that even the application of simple AO systems yields a substantial gain. The systems elaborated at the Institute of Atmospheric Optics can be applied in optical viewing systems and astronomical devices for routine operation.

## References

1. Lukin V P, Pokasov V V *Appl. Opt.* **20** 121 (1981)
2. Lukin V P *Atmosfer'naya Adaptivnaya Optika* (Atmospheric Adaptive Optics) (Novosibirsk: Nauka, 1986) [Translated into English (Bellingham, Wash.: SPIE Press, 1995)]
3. Gubkin S M et al. *Astron. Zh.* **60** 789 (1983) [*Sov. Astron.* **27** 455 (1983)]
4. Lukin V P *Opt. Atm. Okeana* **10** 516 (1997) [*Atm. Oceanic Opt.* **10** 322 (1997)]
5. Nosov V V et al. *Opt. Atm.* **18** 845 (2005) [*Atm. Oceanic Opt.* **18** 756 (2005)]
6. Lukin V P *Opt. Lett.* **4** 15 (1979)
7. Lukin V P, Emaleev O N *Kvantovaya Elektron.* **7** 1270 (1980) [*Sov. J. Quantum Electron.* **10** 727 (1980)]
8. Lukin V P, Matyukhin V F *Kvantovaya Elektron.* **10** 1264 (1983) [*Sov. J. Quantum Electron.* **13** 814 (1983)]
9. Zuev V E, Lukin V P *Appl. Opt.* **26** 139 (1987)
10. Emaleev O N, Lukin V P *Kvantovaya Elektron.* **9** 2264 (1982) [*Sov. J. Quantum Electron.* **12** 1470 (1982)]
11. Lukin V P et al. *J. Opt. Soc. Am. A* **11** 903 (1994)
12. Lukin V P *Proc. SPIE* **2222** 527 (1994)
13. Vitrichenko E A et al. *Problemy Opticheskogo Kontrolya* (Optical Check Problems) (Executive Ed. I V Samokhvalov) (Novosibirsk: Nauka, 1990)
14. Vitrichenko E A et al. *Dokl. Akad. Nauk SSSR* **300** 312 (1988) [*Sov. Phys. Dokl.* **33** 309 (1988)]
15. Fortes B V, Lukin V P *Proc. SPIE* **1688** 477 (1992)
16. Lukin V P et al. *Proc. SPIE* **2222** 522 (1994); *Opt. Atm. Okeana* **8** 409 (1995) [*Atm. Oceanic Opt.* **8** 210 (1995)]
17. Lukin V P, in *Adaptive Optics. Proc. of a Topical Meeting, October 2–6, 1995, Garching, Germany* (ESO Workshop Proc., No. 54, Ed. M Cullum) (Garching bei München: European Southern Observatory, 1996) p. 373
18. Lukin V P, Fortes B V *Astron. Zh.* **73** 419 (1996) [*Astron. Rep.* **40** 378 (1996)]
19. Lukin V P *Opt. Atm. Okeana* **9** 1433 (1996) [*Atm. Oceanic Opt.* **9** 910 (1996)]
20. Lukin V P et al. *Opt. Atm. Okeana* **12** 1161 (1999) [*Atm. Oceanic Opt.* **12** 1107 (1999)]
21. Lukin V P *Appl. Opt.* **37** 4634 (1998)
22. Lukin V P et al. *Opt. Zh.* **73** (3) 55 (2006) [*J. Opt. Technol.* **73** 197 (2006)]
23. Lukin V P, Fortes B V *Adaptivnoe Formirovanie Puchkov i Izobrazhenii v Atmosfere* (Adaptive Beaming and Imaging in the Turbulent Atmosphere) (Novosibirsk: Izd. SO RAN, 1999) [Translated into English (Bellingham, Wash.: SPIE Press, 2002)]
24. Kanev F Yu, Lukin V P *Adaptivnaya Optika. Chislennye i Eksperimental'nye Issledovaniya* (Adaptive Optics. Numerical and Experimental Research) (Tomsk: Izd. Inst. Optiki Atmosfery SO RAN, 2005)